Relation between damping of the hot giant dipole resonance and the complex admittance of an irreversible process

Nguyen Dinh Dang[1,*] and Fumihiko Sakata[2]
[1]*Cyclotron Laboratory, RIKEN, Wako, Saitama 351-01, Japan*
[2]*Department of Mathematical Sciences, Ibaraki University, Mito 310, Japan*
(Received 18 April 1997; revised manuscript received 14 October 1997)

It is shown that the complex admittance, which describes the dissipation of the giant dipole resonance (GDR) in hot nuclei, can be derived from the microscopic double-time Green function for the propagation of the GDR. The damping width of the GDR is calculated directly from the complex admittance without explicitly solving the equation for the poles of the Green function. Using this method, a systematic study of the width of the GDR as a function of temperature T is carried out in ^{120}Sn and ^{208}Pb. The quantal width, caused by the coupling to ph configurations decreases slowly with increasing T. The thermal width, caused by the coupling to pp and hh configurations at $T\neq 0$, increases sharply at low temperatures up to $T\sim$ 3 MeV, and slowly at high temperatures, where it reaches a saturation in the region of $T>$ 3–4 MeV. The calculated values of the total damping width of the GDR are found in reasonable agreement with the experimental data in heavy-ion fusion reactions and inelastic α scattering. The mechanism of the ''disappearance'' of the GDR at high temperatures is analyzed. The evidence of motional narrowing in the hot GDR is investigated. [S0556-2813(98)01906-2]

PACS number(s): 24.30.Cz, 05.70.Ln, 24.10.Pa

I. INTRODUCTION

It is now well-established that the width of the observed giant dipole resonance in hot nuclei (the hot GDR) increases strongly as the excitation energy increases up to around 130 MeV in tin isotopes. At higher excitation energies the width increases slowly and even saturates [1–6]. (See also Refs. [7,8] for the reviews). A considerable number of theoretical studies have been performed in the last decade on the subject of the damping of hot GDR [9–19]. While theories can reproduce the centroid energy of the hot GDR, many of them still give different, sometimes controversial explanations regarding its width. The hot GDR has been observed first in the compound-nuclear reactions induced in heavy-ion collisions [1–6]. In these experiments the hot compound nucleus was usually formed at high angular momentum. The dependence of the width of the hot GDR on the excitation energy E^* contained then both effects of the angular momentum and the temperature T. Recently two new experimental methods have been introduced. The first one involves compound nuclear reactions [20], where large arrays of γ detectors have been set up to measure the GDR of a hot system at a definite angular momentum. The second one [21] is based on a new technique using α particles to excite the target nucleus via inelastic scattering at a small angular momentum. These new methods have offered a possibility to individually study the effects of temperature and of angular momentum on the damping of the hot GDR in a direct comparison with theoretical predictions.

In the microscopic extrapolation to nonzero temperature the conventional approaches to hot GDR have included the effect of temperature via a simple replacement of the average over the ground state at $T=0$ by the one over the thermal statistical ensemble. This means that the hot GDR has been considered as a quantal eigenstate built on top of the thermal equilibrium ensemble. The results show that the average quantities of the system such as the Landau splitting calculated within the self-consistent random phase approximation (SC-RPA) at finite temperature (SC-FTRPA) [12,13] and the spreading width $\Gamma^{\downarrow}$ of the hot GDR, arising after coupling the ph states to $2p2h$ ones [14,15], remain stable against varying T. In order to understand the increase of the observed width of the hot GDR other thermodynamical effects such as thermal fluctuations of shapes, temperature-dependent transferred angular momentum, etc. were introduced [16,17]. Thermal fluctuations have also been taken into account in the recent theory on the hot GDR width [18]. The authors of Ref. [6] have pointed out, however, that the increase of the width, offered by the theory in Ref. [18], is still quite slow in order to account for the experimental systematics. Reference [6], therefore, has called for a search of a missing effect, emphasizing the role played by thermal and angular momentum effects in the low excitation energy region ($E^*\leqslant$ 200 MeV). The most recent theoretical evaluations in Ref. [22], which include the thermal shape fluctuations within an adiabatic model, agree nicely with the α scattering data in Ref. [21] for the GDR width in ^{120}Sn and ^{208}Pb at temperatures 1 MeV $<T\leqslant$ 3 MeV (30 MeV $\leqslant E^*\leqslant$ 130 MeV). The increase of the evaporation width Γ_{ev} due to a finite lifetime of the compound nuclear states [19], has also been included to improve the results at $T\sim$ 3 MeV. The theoretical predictions of Ref. [22] are given for $T\leqslant$3.4 MeV. It is not clear whether the adiabatic model can describe with the same success the region of the width saturation

*Present address: Department of Physics, Faculty of Sciences, Saitama University, 255 Shimo-Okubo, Urawa, 338-8570 Saitama, Japan. Email: dang@rikaxp.riken.go.jp - On leave of absence from the Institute of Nuclear Science and Technique, VAEC, Hanoi, Vietnam.

 © 1998 The American Physical Society

($E^* > 130$ MeV), where a considerable number of heavy-ion fusion data has been accumulated up to $E^* \sim 450$ MeV. These results have also shown that the effects due to angular momentum on the data set of interest are negligible. This observation is important as it confirms the domination of thermal effects in the increase and saturation of the GDR width.

From the macroscopic point of view the GDR built on the ground state ($T = 0$) (the g.s. GDR) can be considered as the Landau zero sound [23]. The damping of the hot GDR has been studied within the framework of the Landau-Vlasov theory (See Refs. [24,25] and references therein). The width of the GDR within this approach shows a continuous increase as the temperature increases. The width saturation at $T \geqslant 3$ MeV and the ''disappearance'' of the GDR at high temperature ($T > 4.5 \sim 5$ MeV), observed in some heavy-ion fusion experiments [26], are interpreted within this approach mainly as a result of an exceedingly large width. In the recent Ref. [27], it has been shown, however, that at $T \geqslant 2$ MeV the regime of rare collisions, where the random phase approximation (RPA) method can be applied in the theory of Fermi liquid, must be replaced with the regime of frequent collisions. Including the memory effects in the collisional integral and the quadrupole distortion of the Fermi surface, the collisional width of the GDR, obtained in Ref. [27], turns out to be rather independent on temperature in an agreement with the predictions of microscopic theories [14,15]. Thermal shape fluctuations have also been taken into account based on the Landau theory of nuclear shape transitions in Ref. [28]. The latter provides a nice macroscopic description of thermal fluctuations in all quadrupole shape degrees of freedom. With all parameters fixed at zero temperature this theory shows good agreement with the data for hot GDR up to $T = 2 \sim 3$ MeV.

In the present situation we see two particularly important issues in the theoretical study of the behavior of the GDR as a function of temperature. The first one is the need of a consistent description of the hot GDR width as a function of temperature, including both regions of the width increase at low temperatures ($0 \leqslant T \leqslant 3$ MeV) as well as of the width saturation ($T \geqslant 3$ MeV) up to the region where the GDR is thought to disappear ($T > 4.5 \sim 5$ MeV). The second one is the connection between the microscopic and macroscopic understandings of the damping mechanism of hot GDR. Recently we have shown in a series of works [29,30] that the coupling of the RPA phonon to the pp and hh configurations, which appear at nonzero temperature, leads to the thermal damping of the collective vibration (phonon). In our most recent work [31] we gave our answer to the first issue. Namely, we have performed a systematic study of the damping of the GDR in ^{90}Zr, ^{120}Sn, and ^{208}Pb as a function of temperature T. The results have shown that the coupling of the collective vibration to the pp and hh excitations, which causes the thermal damping width, is responsible for the increase of the total width with increasing temperature up to $T \approx 3$ MeV and its saturation at higher temperatures. Our results are found in an overall agreement with the experimental data for the GDR width obtained in the inelastic α scattering and heavy-ion fusion reactions at excitation energies $E^* \leqslant 450$ MeV.

In the present paper we will make a further step in this direction by answering the second issue mentioned above. Namely, we would like to study here a connection between the microscopic description and a macroscopic interpretation of the hot GDR. As a result we shall propose an alternative way to estimate the damping width of the GDR via the complex admittance of an irreversible process. This work is organized as follows. In Sec. II we study the dissipation of the hot GDR, considering it as a statistical state, which is slightly deviated from the thermal equilibrium under the influence of a temperature-dependent external perturbation. As a matter of fact, in intermediate-energy heavy-ion collisions the hot GDR can be present as a thermal excitation and the detected γ rays are emitted predominantly in the nonequilibrium phase. The evolution of this weakly nonequilibrium state can be described by the transport equation of a linear irreversible process. An alternative treatment within the time-dependent Hartree-Fock (TDHF) approach can be found in Ref. [32]. However we shall use the double-time Green function method to derive the complex admittance of this process in a microscopic way without explicitly recoursing to the transport equation. The systematic numerical calculations are carried out in realistic nuclei, ^{120}Sn and ^{208}Pb, within a large range of temperature (up to at least $T = 6$ MeV) in Sec. III. The results are compared with the recent experimental data for the hot GDR in these nuclei in heavy ion fusion reactions and inelastic α scattering. The paper is summarized in the last section, where some conclusions are provided.

II. EVOLUTION OF THE HOT GDR IN AN IRREVERSIBLE PROCESS

We consider the dissipation of the hot GDR as a statistical state, which is slightly deviated from the thermal equilibrium under the influence of a temperature-dependent external perturbation. The weakly nonequilibrium state can be constructed, considering the response of a system, which is described by a time-independent Hamiltonian H_h, on an external perturbation H_t^1 [33,34] under the assumption that there is no external perturbation at the time $t = -\infty$. The total Hamiltonian is

$$H = H_h + H_t^1, \quad H_{t=-\infty}^1 = 0. \tag{2.1}$$

The evolution of a dynamical variable $\hat{\mathcal{O}}$, whose average value is $\overline{\mathcal{O}(t)} = \mathrm{Tr}\{\rho(t)\hat{\mathcal{O}}\}$, can be studied in terms of a time-dependent density operator $\rho(t)$. The latter satisfies the von Neumann equation with a condition that at $t = -\infty$ the system is in the thermal equilibrium:

$$i\frac{\partial}{\partial t}\rho(t) = [H_h + H_t^1, \rho(t)],$$

$$\rho(-\infty) = \rho = e^{-\beta H_h}/\mathrm{Tr}\{e^{-\beta H_h}\}, \quad \beta = T^{-1}. \tag{2.2}$$

Since the external perturbation is assumed to be small, Eq. (2.2) can be solved by linearizing the density operator $\rho(t)$ with its first-order (small) increment $\Delta\rho(t)$

$$\rho(t) = \rho + \Delta\rho(t), \tag{2.3}$$

so that $H_t^1 \Delta\rho(t)$ can be neglected. Under these conditions the evolution of the dynamical variable $\hat{\mathcal{O}}$ is described by the equation well-known in the statistical mechanics of irreversible processes [33,34]. With switching on a periodic perturbation, for example, this equation takes the form

$$\overline{\mathcal{O}(t)} = \langle \hat{\mathcal{O}} \rangle + 2\pi \sum_q e^{-i\Omega_q t + \varepsilon t} \langle\langle \hat{\mathcal{O}}; V_q \rangle\rangle^{\rm ret}_{E=\Omega_q}, \quad (2.4)$$

where $\langle \ldots \rangle$ denotes the average over the grand canonical ensemble:

$$\langle \ldots \rangle = {\rm Tr}\{\rho \ldots\} = \frac{{\rm Tr}\{\ldots \exp(-\beta H_h)\}}{{\rm Tr}\{\exp(-\beta H_h)\}}, \quad (2.5)$$

the sum $\Sigma_q V_q \equiv H^1$ is the time-independent part of the external perturbation H_t^1, and Ω_q is the energy of elementary excitations, characterizing the distribution of the wave packet associated with the evolution of the dynamical variable under consideration. The retarded Green function $\langle\langle \hat{\mathcal{O}}; V_q \rangle\rangle^{\rm ret}$, taken at energy $E = \Omega_q$ (the after-effect function), is related to the complex admittance $\chi_q(\Omega_q)$ as [33,34]

$$\chi_q(\Omega_q) = -2\pi \langle\langle \hat{\mathcal{O}}; \hat{V}_q \rangle\rangle^{\rm ret}_{E=\Omega_q}, \quad (2.6)$$

where $\hat{V}_q$ is the operator part of V_q.

In order to estimate microscopically the complex admittance $\chi_q(E)$ in Eq. (2.6) we adopt in Eq. (2.1) a model Hamiltonian, which includes the coupling of collective oscillations (phonons) to the field of ph, pp, and hh pairs in a form of a sum of three terms:

$$H = \sum_s E_s a_s^\dagger a_s + \sum_q \omega_q Q_q^\dagger Q_q + \sum_{ss'q} F_{ss'}^{(q)} a_s^\dagger a_{s'} (Q_q^\dagger + Q_q). \quad (2.7)$$

The first term in the RHS of Eq. (2.7) describes the field of independent single particles $a_s^\dagger$ and a_s. The second term stands for the phonon field $\{Q_q^\dagger, Q_q\}$. The last term represents the coupling between the two fields. $E_s = \epsilon_s - \epsilon_F$, where ϵ_s is the single-particle energy and ϵ_F is the Fermi surface's energy. Hereafter the energy E_s is simply called the single-particle energy. The phonon energy is denoted as ω_q. This form of the model Hamiltonian in Eq. (2.7) is quite general and common in many microscopic approaches to nuclear collective excitations. The difference is in the way of defining the single-particle energy E_s, phonon energy ω_q and phonon structure under a specific effective coupling $F_{ss'}^{(q)}$. In the quasiparticle-phonon model (QPM) [35] or in Ref. [36], e.g., the coupling vertex $F_{ss'}^{(q)}$ is a sum of products of the coupling strength and the coupling-matrix elements. The coupling strength contains the RPA amplitudes of ph configurations in the collective oscillation. The coupling matrix elements can be obtained through the derivative of the central potential. In the QPM, e.g., phonon operators $Q_q^\dagger$ and Q_q have the fermion structure, being built from the coherent ph or quasiparticle pairs. Recently, the form in Eq. (2.7) has been derived rigorously from the QPM Hamiltonian in Ref. [30]. In the simplest case when the two-body term consists of only a separable isovector dipole-dipole interaction, one recovers from Eq. (2.7) the Hamiltonian widely used in the literature to describe the GDR [37]. The term, containing a sum of products of two pp (hh) pairs, is omitted in Eq. (2.7) as it has a little influence on the damping of phonon excitations [38].

We introduce the double-time Green functions [39], which describe the following:

(1) *The propagation of a free particle (or hole)*:

$$G_{s';s}(t-t') = \langle\langle a_{s'}(t); a_s^\dagger(t') \rangle\rangle, \quad (2.8)$$

(2) *The propagation of a free phonon*:

$$G_{q';q}(t-t') = \langle\langle Q_{q'}(t); Q_q^\dagger(t') \rangle\rangle, \quad (2.9)$$

(3) *The particle-phonon coupling in the single-particle field*:

$$\Gamma^-_{s'q;s}(t-t') = \langle\langle a_{s'}(t) Q_q(t); a_s^\dagger(t') \rangle\rangle, \quad (2.10)$$

$$\Gamma^+_{s'q;s}(t-t') = \langle\langle a_{s'}(t) Q_q^\dagger(t); a_s^\dagger(t') \rangle\rangle, \quad (2.11)$$

(4) *The transition between a nucleon pair and a phonon*:

$$\mathcal{G}^-_{ss';q}(t-t') = \langle\langle a_s^\dagger(t) a_{s'}(t); Q_q^\dagger(t') \rangle\rangle. \quad (2.12)$$

The effect of the backward process, described by the Green function $\langle\langle Q_{q'}^\dagger(t); Q_q^\dagger(t') \rangle\rangle$, is small [30], so we neglect it here. In Eqs. (2.8)–(2.12) the standard notation is used for the double-time retarded Green function [33,39]. A set of coupled equations for an hierarchy of Green functions is obtained, applying the standard method of the equation of motion for the double-time Green functions [33,39,40]. We close this hierarchy to the functions in Eqs. (2.8)–(2.12), using a decoupling approximation as described in Refs. [33,39]:

$$\langle\langle a_{s_1} \underbrace{Q_q^\dagger Q_{q'}}; a_s^\dagger \rangle\rangle = \delta_{qq'} \nu_q G_{s_1;s}, \quad \langle\langle a_{s_1} \underbrace{Q_{q'} Q_q^\dagger}; a_s^\dagger \rangle\rangle = \delta_{qq'} (1+\nu_q) G_{s_1;s}, \quad (2.13)$$

$$\langle\langle \underbrace{a_s^\dagger a_{s_1}} (Q_{q'}^\dagger + Q_{q'}); Q_q^\dagger \rangle\rangle = \delta_{ss_1} n_s G_{q';q}, \quad \langle\langle \underbrace{a_{s'} a_{s_1}^\dagger} a_{s_1}; a_s^\dagger \rangle\rangle = \delta_{s's_1} (1-n_{s'}) G_{s'_1;s}. \quad (2.14)$$

In Eqs. (2.13) and (2.14) $n_s=\langle a_s^\dagger a_s\rangle$ and $\nu_q=\langle Q_q^\dagger Q_q\rangle$ are the single-particle and phonon occupation numbers, respectively. The time variable is omitted for simplicity. Making the Fourier transformation to the energy plane E and eliminating then functions $\Gamma^-(E)$, $\Gamma^+(E)$, and $\mathcal{G}(E)$ by expressing them in terms of $G_{s;s'}(E)$ and $G_{q;q'}(E)$, we obtain a set of two equations for $G_{s;s'}(E)$ and $G_{q;q'}(E)$, which describe the p (h) and phonon propagations, respectively. For the propagation of a single p (or h) state $s=s'$ and a single phonon state $q=q'$ these equations have the simple form:

$$G_s(E)=\frac{1}{2\pi}[E-E_s-M_s(E)]^{-1},$$

$$G_q(E)=\frac{1}{2\pi}[E-\omega_q-P_q(E)]^{-1}, \tag{2.15}$$

where the mass $M_s(E)$ and polarization $P_q(E)$ operators are

$$M_s(E)=\sum_{q's'} F_{ss'}^{(q')}F_{s's}^{(q')}\left(\frac{\nu_{q'}+1-n_{s'}}{E-E_{s'}-\omega_{q'}}+\frac{n_{s'}+\nu_{q'}}{E-E_{s'}+\omega_{q'}}\right),$$

$$P_q(E)=\sum_{ss'} F_{ss'}^{(q)}F_{s's}^{(q)}\frac{n_s-n_{s'}}{E-E_{s'}+E_s}. \tag{2.16}$$

Closing the hierarchy to the functions in Eqs. (2.8)–(2.12) restricts the couplings in the single-particle mass operator $M_s(E)$ to at most $2p1h$ configurations if the one-phonon operator generates the collective ph excitation. On the other hand the g.s. GDR acquires the spreading width $\Gamma^\downarrow$ mostly via coupling to $2p2h$ configurations. The latter can be included by extending the hierarchy to higher-order Green functions of ''$1p1h\oplus$phonon'' type $\langle\langle a_h^\dagger(t)a_p(t)Q_q(t);Q_{q'}^\dagger(t')\rangle\rangle$ as in Ref. [14] or two-phonon type $\langle\langle Q_{q_1}(t)Q_{q_2}(t);Q_{q'}^\dagger(t')\rangle\rangle$, etc. as in Ref. [15]. The result would then include the graphs in Figs. 3 and 4 of Ref. [14] or in Fig. 1 of Ref. [15] for the phonon polarization operator $P_q(E)$. The numerical calculations in Refs. [14,15] have shown, however, that the effects of these graphs on the spreading width of the GDR are almost independent of the temperature. Therefore, in order to maintain the simplicity, we will include the spreading due to these effects in the parameters of the model defined at $T=0$ in the next section. The explicit inclusion of these higher-order double-time Green functions is reserved for our forthcoming study.

The dampings $\gamma_s(\omega)$ of the single-particle and $\gamma_q(\omega)$ of the phonon states are derived as the imaginary parts of the analytical continuation in the complex energy plane $\eta=\omega\pm i\varepsilon$ of the mass $M_s(E)$ and polarization operators $P_q(E)$, respectively:

$$\gamma_s(\omega)=\pi\sum_{q's'} F_{ss'}^{(q')}F_{s's}^{(q')}[(\nu_{q'}+1-n_{s'})\delta(\omega-E_{s'}-\omega_{q'})+(n_{s'}+\nu_{q'})\delta(\omega-E_{s'}+\omega_{q'})], \tag{2.17}$$

$$\gamma_q(\omega)=\pi\sum_{ss'} F_{ss'}^{(q)}F_{s's}^{(q)}(n_s-n_{s'})\delta(\omega-E_{s'}+E_s). \tag{2.18}$$

The single-particle occupation number n_s (phonon occupation number ν_q) in Eqs. (2.16)–(2.18) has the form of a Fermi (Bose) distribution, which is folded with a Lorentzian with a width of $2\gamma_s(\omega)$ $(2\gamma_q(\omega))$ and centered at $\tilde{E}_s=E_s+M_s(\tilde{E}_s)$ $[\tilde{\omega}_q=\omega_q+P_q(\tilde{\omega}_q)]$. In Ref. [30] it has been shown in an example of a damped harmonic oscillator that $\gamma_q(\omega)$ is indeed the half-width of the oscillator damping, while the real part of the analytical continuation of the polarization operator $P_q(E)$ into the complex energy plane gives the frequency shift of the damped oscillator. A similar proof can be extended to the single-particle damping width $\gamma_s(\omega)$ in a straightforward manner. If γ_s is small, the single-particle occupation number can be well approximated by an exact Fermi distribution function with energy $\tilde{E}_s$. For the phonon occupation number this is not valid because γ_q is large.

In Ref. [19] it has been proposed that the states of the compound nucleus have a definite lifetime or width. In the most general case, the energy levels of the compound nucleus include both discrete and continuum parts. Since the high-lying bound states of the single-particle spectrum may acquire an appreciable width via the coupling to the continuum, this certainly affects also the single-particle damping γ_s in Eq. (2.17). While the escape width $\Gamma^\uparrow$ is known to be only a small fraction (around few hundreds keV) of the observed width of the GDR in heavy nuclei at $T=0$, its contribution to the total damping of GDR may become significant at very high temperature. The role of the evaporation width Γ_{ev} at $T\neq 0$ has been studied in Refs. [19,22] and also in Ref. [41]. In the latter, it has been suggested that the ''disappearance'' of the hot GDR at very high temperatures may be associated with the growth of the evaporation width Γ_{ev}. Even though the continuum is not explicitly included in our formalism, we can say that the effect of coupling to the continuum can be incorporated here, at least partially, in an effective way. Indeed, as will be discussed in the next section, the numerical calculations in our formalism use the single-particle energy spectra, defined within the Woods-Saxon potential. These spectra include not only the levels near the Fermi surface, but also high-lying bound states and quasi-bound states. Therefore, the poles in Eq. (2.18) can be located at rather high excitation energies in the continuum region. Hence, the effects caused by coupling to these high-lying discrete states can simulate the effect of coupling to the continuum.

If we assume that before the coupling the GDR is generated by a single phonon, associated with a strongly collective

vibration at energy ω_q, the full width at half maximum (FWHM) $\Gamma_{\rm GDR}$ of the GDR, caused by the coupling, is calculated from Eq. (2.18) as

$$\Gamma_{\rm GDR}=2\gamma_q[\omega=E_{\rm GDR}(T)]. \tag{2.19}$$

This width $\Gamma_{\rm GDR}$ must be compared with the FWHM of the GDR, extracted in the experiments. The energy $E_{\rm GDR}(T)$ of the hot GDR is defined as the pole of the Green function $G_q(\omega)$ at the real energy ω from the equation

$$\omega-\omega_q-P_q(\omega)=0. \tag{2.20}$$

The width $\Gamma_{\rm GDR}$ in Eq. (2.19) has been calculated in Ref. [31] for ^{90}Zr, ^{120}Sn, and ^{208}Pb. The results have been found in overall agreement with the experimental data in heavy-ion fusion reactions as well as in inelastic α scattering. The calculations also showed that the effect of single-particle damping on the width of the GDR is rather small up to high temperatures. The increase of the GDR width at low temperatures and its saturation at high temperatures are explained within this model as follows. At $T=0$ the single-particle occupation number n_s is equal to one for a hole state ($E_h<0$) and zero for a particle one ($E_p>0$). Therefore the GDR width $\Gamma_{\rm GDR}$ has a nonzero value only through the coupling to ph pairs, where $n_h-n_p=1$ [Eq. (2.18)]. As the temperature increases, the quantal damping which we denote as Γ_Q decreases as the difference n_h-n_p decreases from one at $T=0$ to zero at $T=\infty$. At the same time there appear the pp and hh configurations because the difference $n_s-n_{s'}\neq 0$ also for $(s,s')=(p,p')$ or (h,h') at $T\neq 0$. The coupling to pp and hh configurations leads to the thermal damping Γ_T [30], which increases first with increasing T. However, because of the factor $n_s-n_{s'}$, the total phonon damping Γ_q will decrease as $O(T^{-1})$ at large T. Therefore, it must reach some plateau within a certain region of temperature. This is a natural explanation for the width saturation of the GDR within the present model.

We would also like to point out a possible connection between the coupling to pp and hh configurations and the the thermal shape fluctuations. In our opinion the coupling to pp and hh configurations may offer an alternative way to take thermal shape fluctuations into account microscopically. To this end, first of all, it is worth noticing that there are several ways to include thermal shape fluctuations. A common way is to use a model, in which the motion of nucleons is described in terms of a deformed oscillator, Woods-Saxon, or cranked Nilsson potential. The residual interaction between nucleons in the intrinsic system can be described by the dipole-dipole force for the GDR case. This scheme has been proposed in Ref. [16], according to which the cross section, averaged over all possible thermal fluctuations of shapes, is given by

$$\langle\sigma(E;E^*)\rangle=\frac{\int P(E^*)\sigma(E;E^*)dD}{\int P(E^*)dD}, \tag{2.21}$$

where the excitation energy E^*, in general, is a function of temperature T, angular momentum I, and deformation parameters β and γ of the system. The probability $P(E^*)$ is proportional to

$$P(E^*)\propto\exp[-F(E^*)/T], \tag{2.22}$$

where $F(E^*)$ is the free energy of the system. The metric dD (volume element) depends on the deformation parameters. In the approach based on the Landau theory of shape transitions [42], the free energy $F(E^*)$ can be expanded in terms of the ''deformation'' parameters α_{lm}, which determine the deviations of the compound nucleus from the spherical shape. Hence the shape fluctuations must include in general the couplings to all possible multipolarities, not only the quadrupole-quadrupole one. The approach in Ref. [42] then concentrated only on the most important deformation—the quadrupole one, which corresponds to the second order in this expansion α_{2m}, and determined an effective free energy as a function of temperature and α_{2m} only. Another way of taking into account thermal shape fluctuations is based on a model using a collective quadrupole plus GDR Hamiltonian to generate the quadrupole deformation at $T=0$ [43]. In this case the mean field of oscillator type is deformed already at $T=0$ with three frequencies ω_i, $(i=x,y,z)$, related to the Hill-Wheeler deformation parameters β and γ [37]. This scheme has been applied in the most recent calculations of thermal shape fluctuations with the adiabatic-coupling model in Ref. [22]. In the present paper only g.s. spherical nuclei are studied. Still the effects of thermal shape fluctuations, being dependent only on temperature, can be considered via the coupling to pp and hh configurations. Indeed, a pp or hh pair operator $B_{ss'}=a_s^\dagger a_{s'}$ can be expanded in the lowest order as a sum of tensor products of ph pair operators: $\Sigma_h[B_{ph}^\dagger\otimes B_{p'h}]_{\lambda\pi}$ if $(s,s')=(p,p')$ or $\Sigma_p[B_{ph'}^\dagger\otimes B_{ph}]_{\lambda\pi}$ if $(s,s')=(h,h')$ [44]. Therefore the coupling of the last term of the Hamiltonian H in Eq. (2.7) can be rewritten, e.g., for the case with $(s,s')=(p,p')$, as

$$H_c\rightarrow H_{BQ}=\sum_{pp'q}F_{pp'}^{(q)}\sum_h[B_{ph}^\dagger\otimes B_{p'h}]_{\lambda\pi}(Q_q^\dagger+Q_q). \tag{2.23}$$

Expressing $B_{ph}^\dagger$ $(B_{p'h})$ in terms of $Q_{q_1}^\dagger$ and Q_{q_1} ($Q_{q_2}^\dagger$ and Q_{q_2}) using the well-known inverse canonical transformation, one obtains

$$H_{BQ}=\sum_{pp'qq_1q_2}F_{pp'}^{(q)}\sum_h[(X_{ph}^{(q_1)}Q_{q_1}^\dagger-Y_{ph}^{(q_1)}Q_{q_1})\otimes(X_{ph}^{(q_2)}Q_{q_2}^\dagger-Y_{ph}^{(q_2)}Q_{q_2})]_{\lambda\pi}(Q_q^\dagger+Q_q). \tag{2.24}$$

Equation (2.24) suggests that if $Q_q^\dagger$ and Q_q are the GDR phonon operators, $\{Q_{q_1}^\dagger, Q_{q_1}\}$ and $\{Q_{q_2}^\dagger, Q_{q_2}\}$ can have the moment and parity as $(1^-, 2^+)$, $(2^+, 3^-)$, etc. so that the total coupled momentum is again equal to $\lambda^\pi = 1^-$. The RPA amplitudes $X_{ph}^{(q_1)}$, $Y_{ph}^{(q_1)}$, and $X_{ph}^{(q_2)}$, $Y_{ph}^{(q_2)}$ can be calculated microscopically using the residual interactions, which include dipole-dipole, quadrupole-quadrupole, octupole-octupole, etc., forces. This can be seen clearly when the residual interactions are separable. In this case the coupling vertex $F_{ss'}^{(q)}$ in Eq. (2.7) can be evaluated in terms of the RPA amplitudes with multipolarity λ as [30]:

$$F_{ss'}^{(\lambda)} = \frac{k^{(\lambda)}}{4(2\lambda+1)} f_{j_s j_{s'}}^{(\lambda)} \sum_{j_1 j_1'} f_{j_1 j_1'}^{(\lambda)} (X_{j_1 j_1'}^{(\lambda i)} + Y_{j_1 j_1'}^{(\lambda i)}), \quad (2.25)$$

with $k^{(\lambda)}$ being the parameter of the multipole-multipole interaction (details can be found in Ref. [35]). This means that the coupling to pp and hh configurations in the last term of Eq. (2.7) or in H_{BQ} in Eq. (2.24) in fact already includes, via multiphonon configuration mixing at $T \neq 0$, the coupling to different multipole-multipole fields. Taking into account the high-lying ph, pp, and hh configurations, as has been discussed above, the coupling to high-lying multiphonon states is also incorporated in our formalism. It is well-known that the configuration mixing of $1p1h$ with $2p2h$ states [35,49] [or ph with phonon ones discussed above (cf. also Ref. [36])] is decisively important to account for the spreading width $\Gamma^\downarrow$. In addition to the quantal coupling to ph configurations, a quite similar mechanism takes place at $T \neq 0$ via the coupling to pp and hh configurations. As the latter takes place only at $T \neq 0$, it is tantamount to the thermal effects in the fluctuations of multipole deformations of nuclear shapes around the spherical one.

In the present paper we are going to find an alternative way for estimating the damping of the GDR through the complex admittance of an irreversible process. The complex admittance in Eq. (2.6) for the case with $\hat{\mathcal{O}} = Q_q$ can be expressed in terms of the Green function $G_q(E)$ defined in Eq. (2.15). After some simple derivations we obtain

$$\chi_q(E) = -2\pi G_q(E) = -\frac{1}{E - \omega_q - P_q(E)}. \quad (2.26)$$

Equation (2.26) is the microscopic expression of the complex admittance in terms of the energy ω_q of the collective vibration, corresponding to the GDR excitation, and of the polarization operator $P_q(E)$, characterizing the damping of the collective phonon. The information about the transport equation (2.4) is now defined by the real and imaginary parts of the complex admittance [Eq. (2.26)] (in the complex energy plane), from which the imaginary part is directly related to the strength function $S_q(\omega)$ of the hot GDR, namely

$$\mathrm{Im}[\chi_q(E = \omega + i\varepsilon)] = \frac{\gamma_q(\omega) + \varepsilon}{[\omega - \omega_q - P_q(\omega)]^2 + (\gamma_q(\omega) + \varepsilon)^2} \simeq \pi S_q(\omega) \quad \text{if} \quad \varepsilon \ll \gamma_q, \quad (2.27)$$

where

$$S_q(\omega) = \frac{1}{\pi} \frac{\gamma_q(\omega)}{[\omega - \omega_q - P_q(\omega)]^2 + \gamma_q^2(\omega)}. \quad (2.28)$$

Knowing the complex admittance [the Green function $G_q(E)$], one can derive the spectral intensity of the GDR excitation from the relation

$$G_q(\omega + i\varepsilon) - G_q(\omega - i\varepsilon) = -i(\exp^{\omega/T} - 1) J_q(\omega), \quad (2.29)$$

which is equal to [39]

$$J_q(\omega) = S_q(\omega)(\exp(\omega) - 1)^{-1}. \quad (2.30)$$

The normalized relaxation function $\Psi(t)$, associated with the energy dissipation of the GDR to noncollective degrees of freedom in the single-particle field (the heat bath), is defined from the complex admittance after a Fourier transformation as [34]

$$\frac{\chi_q(E)}{\chi_q(0)} - 1 = iE \int_0^\infty \Psi(t) e^{iEt} dt. \quad (2.31)$$

If the corresponding probability $|\Psi(t)|^2$ displays a good exponential decaying behavior

$$|\Psi(t)|^2 = e^{-t/\tau_c} = e^{\Gamma t}, \quad \Gamma = \frac{1}{\tau_c}, \quad (2.32)$$

the width Γ of the GDR strength distribution can be extracted as the reverse of the relaxation time τ_c. Hence, we have found an alternative way to estimate the width of the GDR without calculating directly $\gamma_q(\omega)$ in Eq. (2.18). This means we can avoid directly solving Eq. (2.20), which is much more complicated, especially when the number of collective phonons are not small. Moreover, the detail information of each fragmented excitation would not have much sense since we are interested only in the average or gross structure of the hot GDR. In confronting the calculated value to the experimental data the attention must be paid to the following point. As has been mentioned above, the GDR width was usually extracted in experiments as the FWHM of a Lorentzian, which is centered at the GDR energy and must be compared to the width Γ_{GDR}, calculated in Eq. (2.19). In terms of the complex admittance, this means the width Γ_{GDR} must be extracted from the relaxation function $\Psi_{\mathrm{GDR}}(t)$ [Eq. (2.31)], which is calculated in turn from the complex admittance $\chi_{\mathrm{GDR}}(\omega)$ according to the equation

$$\chi_{\mathrm{GDR}}(E) = -2\pi G_{\mathrm{GDR}}(E) = -\frac{1}{E - E_{\mathrm{GDR}} - P_{\mathrm{GDR}}},$$
$$P_{\mathrm{GDR}} = P_q(\omega = E_{\mathrm{GDR}}), \quad (2.33)$$

instead of Eq. (2.26). In the present model, where the effects of coupling to more complicated configurations such as $2p2h$ ones are incorporated in the parameters, the result from Eq. (2.33) is more reliable than the width Γ from the total strength function. In the next section we will represent the results of calculations of both quantities: the width Γ [Eq. (2.32)] of the total dipole strength distribution over the

whole energy interval up to 40 MeV and the width $\Gamma_{\rm GDR}$ using the complex admittance in Eq. (2.33).

The present formalism can be also used to examine the evidence of motional narrowing in the hot GDR. The application of the theory on motional narrowing [34] to the hot GDR is given in the Appendix. It is shown in the Appendix that motional narrowing would occur in the long-time (sudden) limit when the effective half-width $\tilde{\gamma}$ of the stochastic frequency modulation in Eq. (A25) became much narrower than the frequency spread Δ (the standard deviation of the Gaussian distribution) in the adiabatic (short-time) limit. This is possible if the following criteria hold:

(i) The adiabaticity parameter is much less that 1:

$$\eta = \frac{\Delta}{\Gamma_{\rm GDR}} \ll 1. \tag{2.34}$$

(ii) The frequency spread Δ decreases with increasing temperature T.

(iii) The effective half-width

$$\gamma_{\rm eff} = \eta\Delta \tag{2.35}$$

decreases as increasing temperature T, starting from a certain value T_c. The value T_c would then denote the lower limit of the temperature region where motional narrowing took place.

Even though several efforts have been undertaken to search for the evidence of motional narrowing in the hot GDR [45–47], it is still debated whether this effect is indeed present in realistic situations. The advantage of the present approach as compared to the adiabatic model [46] and the macroscopic approach [47] is that the parameter η can be evaluated microscopically rather than being adjusted to fit the experimental width as in Refs. [46,47]. The present approach is also free from the adiabaticity limitation. The frequency spread Δ in Eqs. (2.34) and (2.35) is determined in terms of the polarization operator $P_q(\omega)$ [Eq. (2.20)] as

$$\Delta = \sqrt{\langle P_q^2(\omega)\rangle} = \sqrt{\frac{\int_0^\infty P_q^2(\omega) S_q(\omega) d\omega}{\int_0^\infty S_q(\omega) d\omega}}. \tag{2.36}$$

Therefore, examining the temperature dependence of η and $\tilde{\gamma}$, we hope to be able to clarify the issue related to motional narrowing in hot GDR within the present formalism.

It is worth emphasizing that the obtained results are physically different from those of the conventional SC-FTRPA, which considers the pp and hh configurations at finite temperature as elementary excitations as the ph ones. The pp and hh configurations in the SC-FTRPA, therefore, participate in forming the collective motion (phonon). As the FTRPA is in fact a one-phonon approximation, the higher-order effects, related to the thermal shape fluctuations and coupling to more complicate configurations, are averaged out of the FTRPA. The remaining part is only some Landau splitting, which is almost independent on temperature as has been mentioned in the Introduction [12,13]. In our formalism, the pp and hh configurations are expressed in terms of noncollective degrees of freedom and they do not participate in constructing the collective vibrational modes. Therefore, they are treated *beyond* the ph FTRPA, if the latter is used to define the microscopic structure of the collective phonon. Under this treatment they induce an irreversible coupling of the collective phonon to the noncollective subspace. In realistic nuclei the number of pp and hh configurations is large. If the average single-particle damping width $\Gamma_{\rm s.p.}$ is small, which is actually the case, the pp and hh configurations can be well approximated by a heat bath. Hence the coupling between the collective phonon and the pp and hh configurations is a de facto GDR-heath bath coupling. The increase of the anharmonicities in the coupling of the collective dipole mode with noncollective states when the temperature increases has also been a decisive feature in the TDHF description of the hot GDR in ^{40}Ca in Ref. [32].

III. NUMERICAL RESULTS

In this section we present the results of the calculations of the GDR width for ^{120}Sn and ^{208}Pb as a function of temperature in a wide range $0 \leqslant T \leqslant 6$ MeV. The results are compared with the experimental data of the GDR's width in heavy-ion fusion reactions and inelastic α scattering. Since we are interested in the evolution of the hot GDR via its coupling to the single-particle field, we assume that the microscopic description of the structure of the g.s. GDR ($T=0$) and its spreading width $\Gamma^{\downarrow}$ is known. Such a description can be found in a number of works such as Refs. [35,36,48,49]. The microscopic calculations at $T \neq 0$ [12–15] have also shown that the GDR can be considered as a strongly collective excitation, which is stable against changing the temperature. Therefore, in order to have a simple and clear picture, we assume that the g.s. GDR can be generated by a single collective and structureless phonon width energy ω_q closed to the energy $E_{\rm GDR}$ of the g.s. GDR. This GDR phonon is damped via coupling to ph, pp, and hh configurations. We employ the realistic single-particle energies, calculated in the Woods-Saxon potential at $T=0$ for ^{90}Zr, ^{120}Sn, and ^{208}Pb. The parameters of the Woods-Saxon potentials have been defined in Ref. [50]. In ^{208}Pb we replace the levels near the Fermi surface with the empirical ones. These energies are extended to nonzero temperatures. The self-consistent calculations in Ref. [51] have shown that the dependence of the single-particle energies on the temperature is rather weak up to $T \simeq 5 \sim 6$ MeV. The matrix elements of the coupling to ph and pp or hh are parametrized as $F_{ph}^{(q)} = F_1$ for $(s,s') = (p,h)$ and $F_{pp}^{(q)} = F_{hh}^{(q)} = F_2$ for $(s,s') = (p,p')$ or (h,h'). As the ph interaction in the GDR is dominated only across the two major shells, which are closest to the Fermi surface from both sides, the uniform distribution of the ph strength over all the levels can be justified if $F_1^2 \ll F_2^2$. The phonon energy ω_q, F_1, and F_2 are three parameters in our model. Their values are chosen for each nucleus so that the empirical quantal width Γ_Q and energy $E_{\rm GDR}$ of the g.s. GDR in these nuclei [52] are reproduced after the coupling is switched on, and that the $E_{\rm GDR}(T)$, defined from Eq. (2.20), does not change appreciably with varying temperature. Reference [37] has shown that this kind of selection of parameters already include the vibration of protons against neutrons in the collective phonon, which generates the g.s. GDR. On the other hand, the coupling to

TABLE I. Parameters of the model used in calculations.

	ω_q (MeV)	F_1 (MeV)	F_2 (MeV)
^{120}Sn	17.0	0.313	1.02
^{208}Pb	13.8	0.103	0.548

$2p2h$ configurations, which leads to the microscopic temperature-independent spreading width $\Gamma^{\downarrow}$, is effectively included in the parameter F_1. The best sets of parameters for ^{120}Sn and ^{208}Pb are presented in the Table I. These values are kept unchanged throughout the calculations at $T \neq 0$. This ensures that all thermal effects are caused by the microscopic coupling between the GDR and the single-particle field, but not by changing parameters. The δ functions in the RHS of Eqs. (2.17) and (2.18) are replaced in numerical calculations with a Lorentzian with a width ε. We have checked and found that the results of calculations do not vary appreciably in the interval 0.2 MeV$\leqslant\varepsilon\leqslant$1.0 MeV. The results, obtained with $\varepsilon = 0.5$ MeV, are discussed below.

Shown in Figs. 1–3 is the imaginary part Im$[\chi_q(E)]$ [Eq. (2.27)] of the complex admittance $\chi_q(E)$, divided by π, for the GDR in ^{120}Sn at several temperatures. The results in Fig. 1 are obtained via coupling to all ph, pp, and hh configurations. Figure 2 represents the results of the calculations, which include only the coupling to ph configurations. In Fig. 3 the results, obtained via coupling to pp and hh configurations, which appear at $T \neq 0$, are displayed. The effect of single-particle damping [Eq. (2.17)], although small, is included in the calculations. These figures show that the GDR bump in a realistic nucleus is a superposition of many Lorentzians. The quantal effects due to the coupling to ph

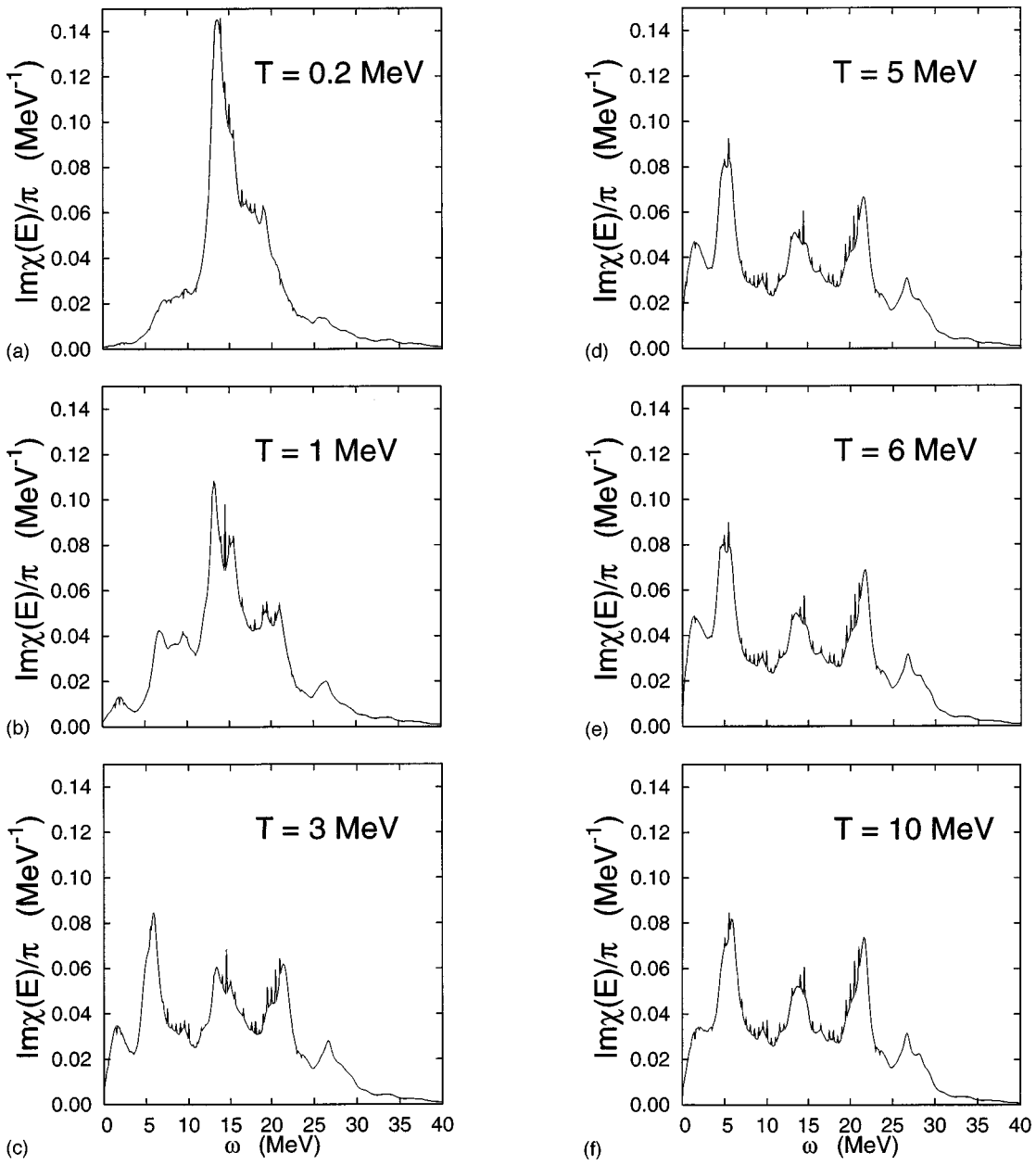

FIG. 1. Imaginary part of the complex admittance of the GDR in ^{120}Sn at several temperatures: Results obtained via the coupling to all ph, pp, and hh configurations.

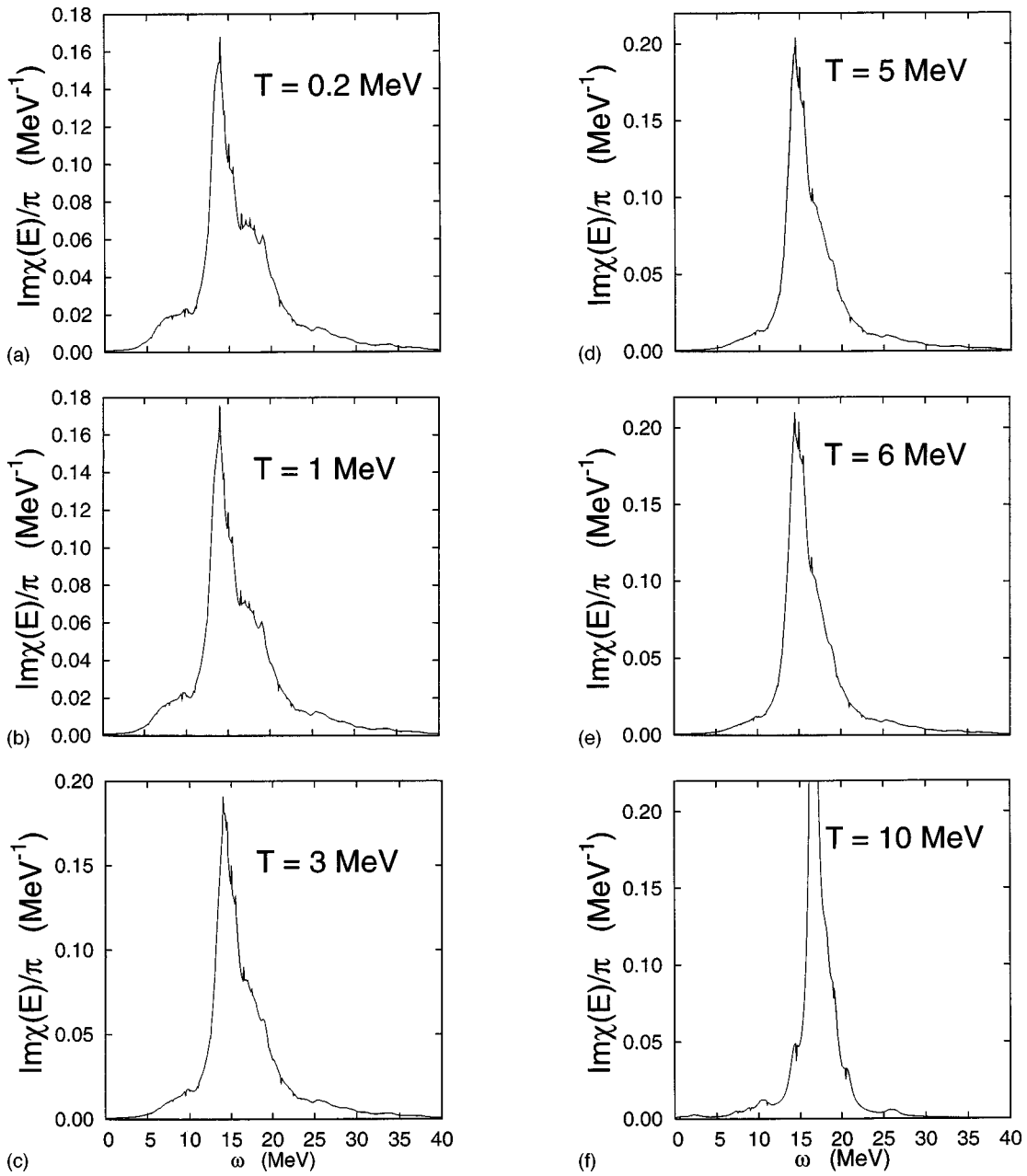

FIG. 2. Imaginary part of the complex admittance of the GDR in ^{120}Sn at several temperatures: Results obtained via the coupling to only *ph* configurations.

configurations (Fig. 2) are getting weaker with increasing temperature. As the result the GDR bump becomes narrower until its width Γ_Q vanishes at high temperatures. At the same time the thermal effects due to the coupling to *pp* and *hh* configurations (Fig. 3) enlarge the GDR as the temperature goes up. Higher than $T\sim$ 3–4 MeV the gross structure of the GDR, caused by thermal effects alone, ceases to change. The combined effects (Fig. 1) give a gross structure of GDR, which changes drastically with increasing T up to 3–4 MeV, but becomes temperature-independent at higher T, conserving the Thomas-Reiche-Kuhn (TRK) sum rule for the GDR. Already in Ref. [30], it has been shown in a simplified model, that there is an energy dissipation from the bump in Fig. 2 to the one in Fig. 3. We can see here that the realistic situation is driven by the same mechanism. The difference is that the space of *pp* and *hh* configurations in realistic hot nuclei is significantly larger and spreads up to high energies, including the GDR region and above it. This makes the GDR persist even up to very high temperature with all its strength preserved. As a matter of fact, we also show in these figures the case with $T=$ 10 MeV to demonstrate that the behavior of the hot GDR becomes insensitive to the change of temperature at $T>$ 3 MeV within this model, even though the maximum temperature a realistic finite system could sustain is about $T\simeq$ 5–6 MeV. As seen from the figures, a pronounced structure in the low energy region, which spreads up to around $\omega=$ 10 MeV, is developed at $T\geqslant$ 2 MeV. On the other hand, a part of the GDR strength is shifted to the higher-energy wing. As the result, the centroid energy of the GDR remains almost unchanged with varying the temperature. As has been pointed out in Ref. [30], the appearance of the low-lying structures may serve as the origin of the ''dis-

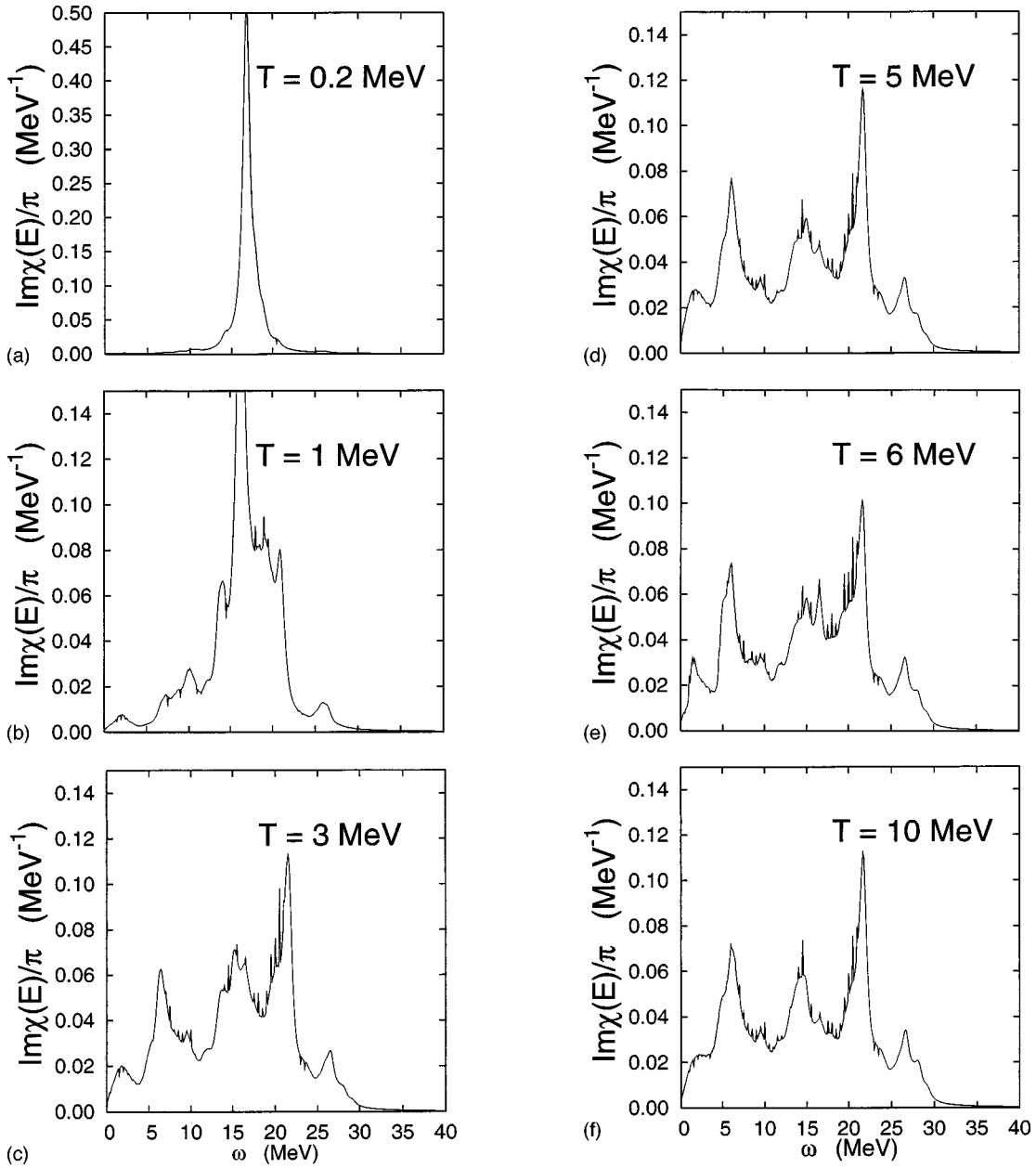

FIG. 3. Imaginary part of the complex admittance of the GDR in ^{120}Sn at several temperatures: Results obtained via the coupling to pp and hh configurations.

appearance'' of the GDR at high excitation energy in some experiments [26]. In fact, these calculations show that it is hard to isolate such low-lying structures when subtracting the exponential background in the experimental spectra. If this is the case, the remaining part can be taken as a GDR with less collectivity or even as a disappearing GDR. Hence, the hot GDR does not seem to disappear within the present model. This result must be understood in the context that the damping mechanism of the GDR at high temperatures comes mainly from thermal effects via the coupling to pp and hh configurations. The quantal effects are due to coupling to ph states, which are responsible for the damping of the g.s. GDR as the zero sound vanishes at high temperatures. This confirms the feature, which has been pointed out in our previous work [30], that as the temperature increases, the possibility for the development of pure quantal collective excitations, such as the coherent motion of all protons against all neutrons, is reduced, vanishing completely at $T\sim$ 5–6 MeV because of the increase of stochastic motion of noncollective degrees of freedom constituting the heat bath. A similar conclusion has been given in Ref. [32] within the TDHF approach, which shows a possibility for a rapid loss of collectivity of the isovector dipole mode due to the growing disorder in the motion of protons against neutrons. These results are similar to those obtained from directly solving Eq. (2.20). The strength function $S_q(\omega)$ in Eq. (2.28), calculated based on this solution with the coupling to all ph, pp, and hh configurations taken into account, is presented in Fig. 4. Comparing this figure with Fig. 1, one can see that they indeed give the same gross structure of the GDR strength distribution at various temperatures. The fine structure is smoother in Fig. 1. The reason is that the calculations of the imaginary part of the complex admittance in Fig. 1 with the same parameter ε have resulted in a stronger smearing as

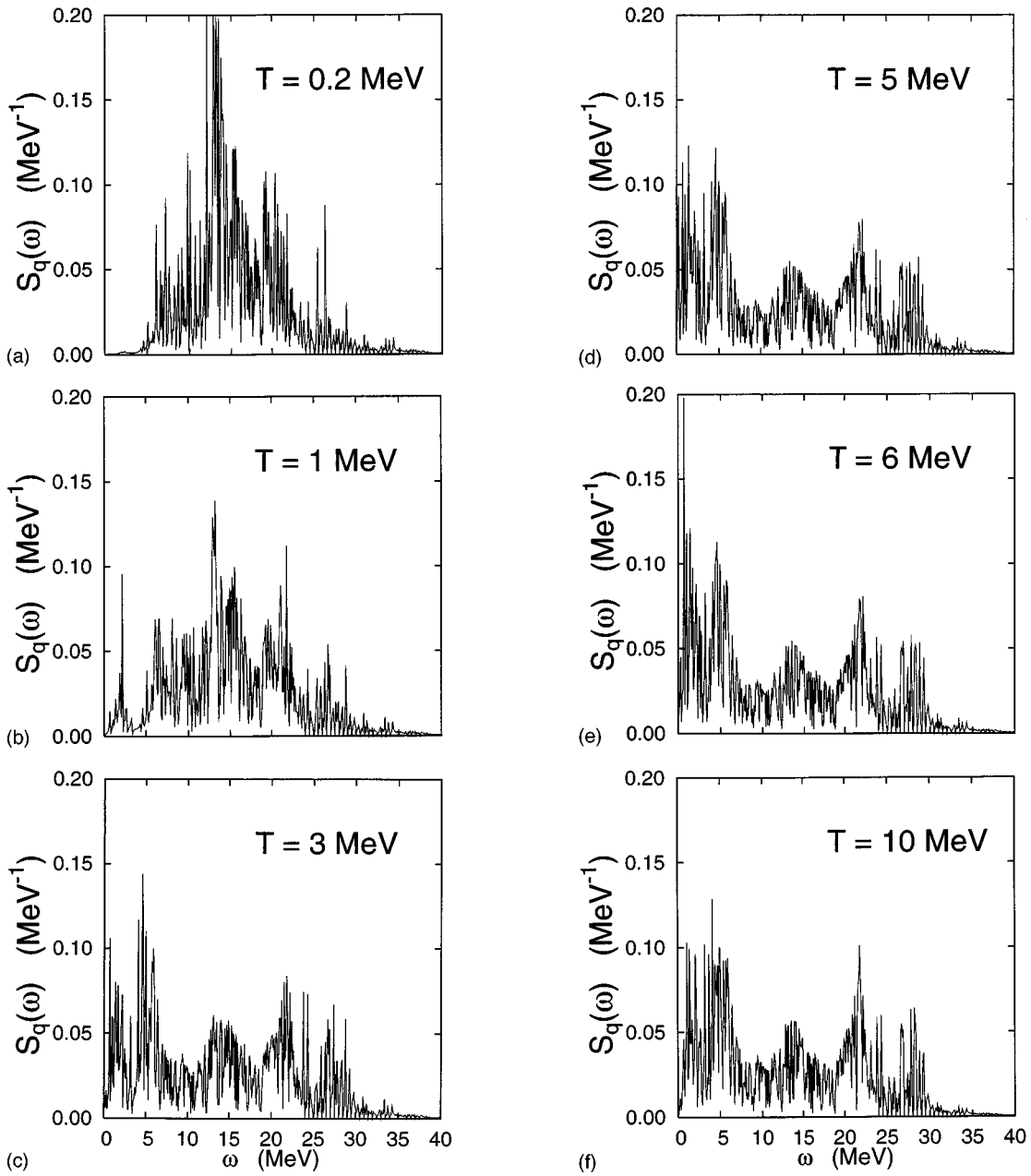

FIG. 4. Strength function of the GDR in ^{120}Sn, calculated from the poles of the Green function $G_q(\omega)$ via the coupling to all ph, pp, and hh at several temperatures.

compared to the strength function $S_q(\omega)$ [Compare Eqs. (2.27) and (2.28)].

Shown in Fig. 5 are the probabilities $|\Psi(t)|^2$ (upper figures) and $|\Psi_{\rm GDR}(t)|^2$ (lower figures), deduced from the complex admittances $\chi(E)$ [Eq. (2.26)] and $\chi_{\rm GDR}(E)$ [Eq. (2.33)], respectively. They are plotted as a function of $1/t$ so that the abscissa of the crossing point between them and the horizontal line $\exp(-1)$ is just equal to the value of the extracted width $1/\tau_c=\Gamma$ (upper figures) or $\Gamma_{\rm GDR}$ (lower figures) at a given temperature. Another way of plotting these figures as a function of t instead of $1/t$ would reveal an obvious exponential decay of functions $|\Psi(t)|^2$ and $|\Psi_{\rm GDR}(t)|^2$. Figures 5(a) and 5(b) represent the results obtained in ^{120}Sn, while Figs. 5(c) and 5(d) show the results in ^{208}Pb at various temperatures. The total width of the GDR obviously increases sharply with increasing temperature T up to 2–3 MeV, but slowly at $T>3$ MeV. It reaches a saturation at $T\sim$ 4–6 MeV.

The width of the GDR, extracted from Fig. 5, and its components in ^{120}Sn and ^{208}Pb are displayed as a function of temperature in Fig. 6(a) and 6(b) in comparison with the recent inelastic α scattering data [21]. The quantal width Γ_Q (dashed curve) is obtained through the coupling to only ph states. The thermal width Γ_T (solid curve) comes from the coupling to pp and hh configurations at $T\neq 0$. The total width $\Gamma_{\rm GDR}$ (solid with diamond curve) is calculated through the coupling to all ph, pp, and hh configurations, including the effect of single-particle damping. The width Γ of the total dipole strength distribution in Fig. 1 is represented by the dotted curve. In general, $\Gamma_{\rm GDR}$ is not the sum of Γ_Q and Γ_T because the poles of the Green function $G_q(\omega)$ are different due to the coupling to different configurations. It is

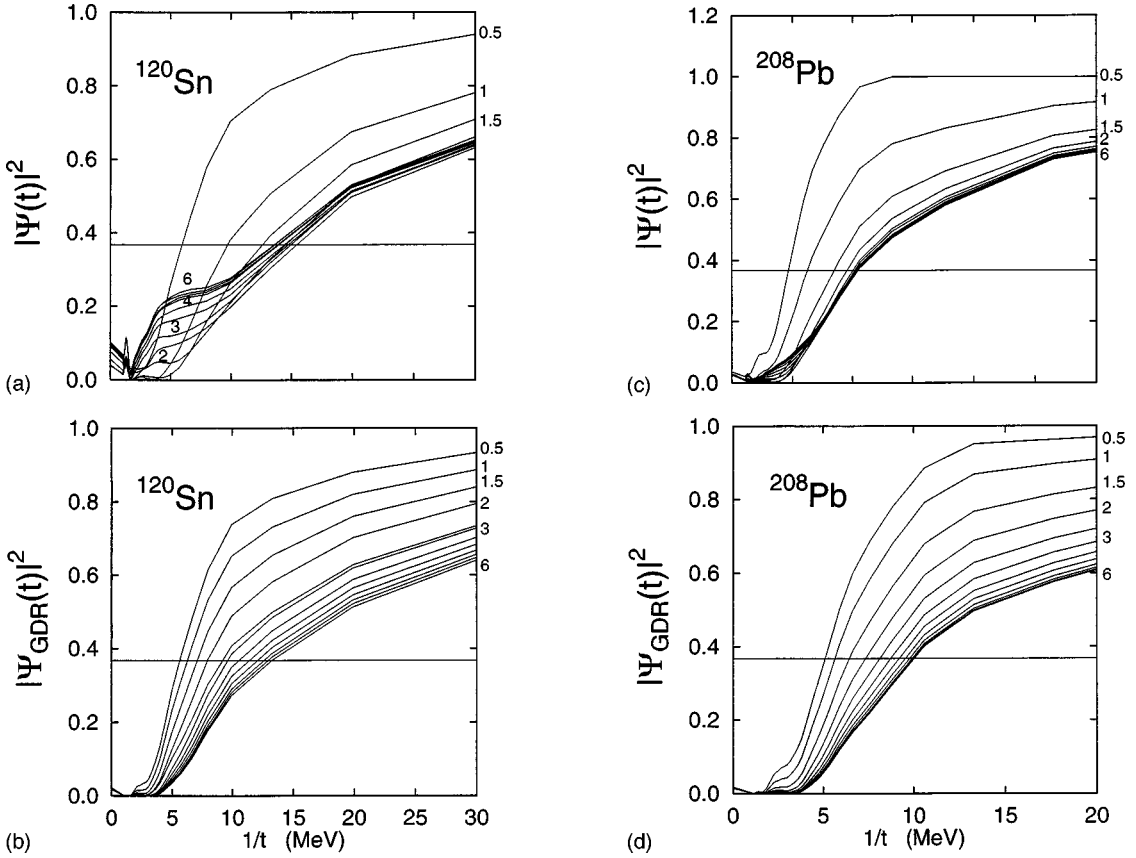

FIG. 5. Probabilities $|\Psi(t)|^2$ (upper figures) and $|\Psi_{\mathrm{GDR}}(t)|^2$ (lower figures) for the GDR in ^{120}Sn (a), (b) and ^{208}Pb (c), (d) as a function of the inversed time $1/t$ at various temperatures. The value of temperature (in MeV), at which a curve was calculated, is given by a number near the curve. The horizontal line is $\exp(-1)$.

clear from this figure that the quantal effect is getting weaker in hot GDR as Γ_Q is slowly getting smaller with T going up. The thermal damping width Γ_T, on the contrary, becomes rapidly larger with increasing T. As the result, Γ_{GDR} increases sharply as T raises up to 3 MeV and slowly at higher temperatures. It reaches a saturated value of around 13.5 MeV in ^{120}Sn and 10 MeV in ^{208}Pb at $T=$ 4–6 MeV. These evaluations also show that the GDR width at higher temperatures is driven mostly by the thermal width Γ_T. The results of our calculations for Γ_{GDR} are in reasonable agreement with the experimental data. This agreement is as good as the one given recently within the adiabatic model in Ref. [22]. Our results also cover a much wider temperature region. It is also seen that the width Γ of the total dipole strength distribution over the whole interval from 0 up to 40 MeV is found in a large discrepancy with the experimental data. In both nuclei the width Γ increases much more rapidly at low temperatures and reaches the saturation at a lower temperature $T\sim$ 2.5 MeV as compared to the width Γ_{GDR}. The reason for this discrepancy is a consequence of the fact that the effect of coupling to $2p2h$ configurations is incorporated in the present model via choosing the parameter F_1 to reproduce the empirical value of the quantal width Γ_q of the g.s. GDR. Therefore, while the value Γ_{GDR} is good as an average one for comparing with the experimental data, the configuration mixing in the calculated strength function is fairly coarse in order to be well approximated by a single Lorentzian as it is the case in the experiments. This result just confirms the fact that the experiments have approximated the hot GDR as a single Lorentzian, centered at the GDR energy $E_{\mathrm{GDR}}(T)$, which just coincides with the theoretical value Γ_{GDR}. On the other hand, it is experimentally difficult to extract the width Γ of the total dipole strength distribution at $T\geqslant$ 3 MeV because of the ambiguities in isolating the low-lying structure from the background at high temperatures, as has been discussed above (Figs. 1 and 4). This may also serve as an explanation of why some authors have considered the saturation of the GDR width as the signature of the GDR disappearance.

Shown in Fig. 6(c) is the same width Γ_{GDR} for ^{120}Sn (a), but plotted as a function of excitation energy E^* in comparison with the FWHM of the GDR from the heavy-ion fusion data in tin isotopes [1–6]. An overall agreement between the theory and experimental data is seen in the whole region of excitation energy E^*, including the data at $250\leqslant E^*\leqslant 450$ MeV [2]. The predictions of Refs. [18] (solid curve) and [24] (dotted curve) are also shown. They are similar to ours at $E^*\leqslant$ 150 MeV. In this region there is a noticeable discrepancy between the dependence of Γ_{GDR} on the excitation energy $E^*_{\mathrm{m.f.}}$, evaluated in the thermal mean-field (solid with diamonds) (see Ref. [53] for details), and the one on $E^*_{\mathrm{F.g.}}$ from the Fermi-gas model with the level density parameter $a=A/12$ (dashed). The contribution of higher-multipole collective vibrations also affect the excitation energy in the thermal mean-field [53]. As the result, $E_{\mathrm{m.f.}}$ is pushed closer to $E_{\mathrm{F.g.}}$. Therefore we also plot in Fig. 6(c) the same width as a function of $\overline{E}^*=(E^*_{\mathrm{m.f.}}+E^*_{\mathrm{F.g.}})/2$ for comparison (solid curve with asterisks).

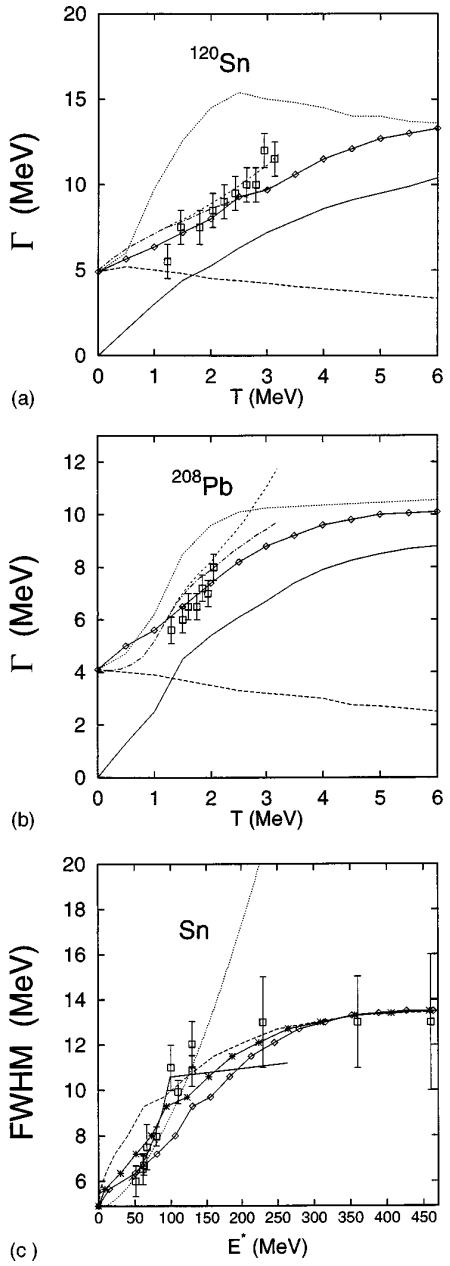

FIG. 6. Widths of the GDR as a function of temperature in ^{120}Sn (a) and ^{208}Pb (b), and as a function of excitation energy in ^{120}Sn (c). The open squares represent the experimental data from inelastic α scattering [(a) and (b)] and heavy-ion fusion reactions (c). In (a) and (b), the solid curves with diamonds denote the width $\Gamma_{\rm GDR}$, calculated at the GDR energy with the coupling to all ph, pp, and hh taken into account. The quantal width Γ_Q, obtained via coupling to only ph configurations, is denoted by the dashed curve, while the thermal width Γ_T, caused by coupling to pp and hh configurations, is represented by the solid curve. The dotted curves represent the width Γ of the total strength function from Fig. 1. The GDR widths, evaluated in Ref. [22] without and including the evaporation width, are shown by the dash-dotted and short dashed curves, respectively. In (c), the solid curve with diamonds represents the width $\Gamma_{\rm GDR}$ in (a), plotted as a function of $E^*_{\rm m.f.}$ (see text). The dashed curve is the same width, but plotted as a function of $E^*_{\rm F.g.}$ from Fermi-gas model. The solid curve with asterisks is the same width, plotted as a function of $\bar{E}^*$ (See text). The width, obtained in Ref. [18], is represented by the solid curve, while the result of Ref. [24] is shown by the dotted curve.

Finally, using criteria (i)–(iii), let us examine whether there is an evidence of motional narrowing in the temperature dependence of the hot GDR. We have calculated the adiabaticity parameter η, the frequency spread Δ, and the effective half-width $\gamma_{\rm eff}$, using Eqs. (2.34), (2.36), and (2.35), respectively, in ^{120}Sn and ^{208}Pb. The results are plotted as a function of temperature in Fig. 7. Starting from $T \geqslant 1.5$ MeV in ^{120}Sn and $T \geqslant 1$ MeV in ^{208}Pb, the value of η, calculated via coupling to pp and hh configurations [solid curves in the top part of Fig. 7], becomes continuously smaller than one and decreases with increasing T. This means that criterion (i) is fulfilled, although not so strongly. This criterion is also fulfilled with the values of η, calculated via couping to only ph configurations (dashed curves in the top figures), or to all ph, pp, and hh ones (solid curves with diamonds in the top figures). In order to see the source of motional narrowing, we have to examine the behavior of the frequency spread Δ [criterion (ii)] and the effective half-width $\gamma_{\rm eff}$ [criterion (iii)]. Taking into account the coupling to pp and hh configurations, Δ continuously increases in general with increasing temperature (solid curve in the middle figures). This means that thermal fluctuations of shapes are not associated with motional narrowing. At the same time, the value of Δ, calculated via coupling to ph configurations (dashed curves in the middle figures), continuously decreases as T goes up, showing a clear effect of motional narrowing with the fulfillment of criterion (ii). This effect has a direct connection with the narrowing of the quantal width Γ_Q as T increases, as has been discussed previously. It is stronger in ^{208}Pb. As a result, the value of Δ, calculated via coupling to all ph, pp, and hh configurations, behaves differently in two nuclei, namely it increases in ^{120}Sn, and slightly decreases (at $T \geqslant 1.5$ MeV) in ^{208}Pb with increasing T. The resulting effective half-width $\gamma_{\rm eff}$ of the stochastic frequency modulation of the hot GDR, shown in the bottom part of Fig. 7, decreases continuously with increasing T when the coupling to only ph configurations (dashed curves) is taken into account. This decrease is also seen in the thermal fluctuations of the hot GDR (solid curves) at $T \geqslant 1$–2 MeV. The resulting effective half-width $\gamma_{\rm eff}$, calculated via coupling to all ph, pp, and hh configurations, starts to decreases at $T \geqslant 1$ MeV in ^{120}Sn and at $T \geqslant 1.5$ MeV in ^{208}Pb. From this analysis we conclude that motional narrowing in the stochastic modulation of the GDR energy (frequency modulation of the hot GDR) indeed takes place at $T \geqslant 1$–1.5 MeV and this effect comes from the quantal coupling to ph configurations [criteria (iii)]. Thermal effect due to coupling to pp and hh configurations (thermal shape fluctuations) are not associated with motional narrowing [criteria (ii) is not fulfilled] and can be considered as an adiabatic process at $T \leqslant 1$ MeV where $\eta > 1$. In general, the behavior of the hot GDR at high temperatures can be approximated by the long-time (sudden time) limit where criterion (i) holds.

IV. CONCLUSIONS

In the present paper we have proposed an alternative method to calculate the damping width of the hot GDR via the complex admittance of an irreversible process. The relation is established between the microscopic theory for the

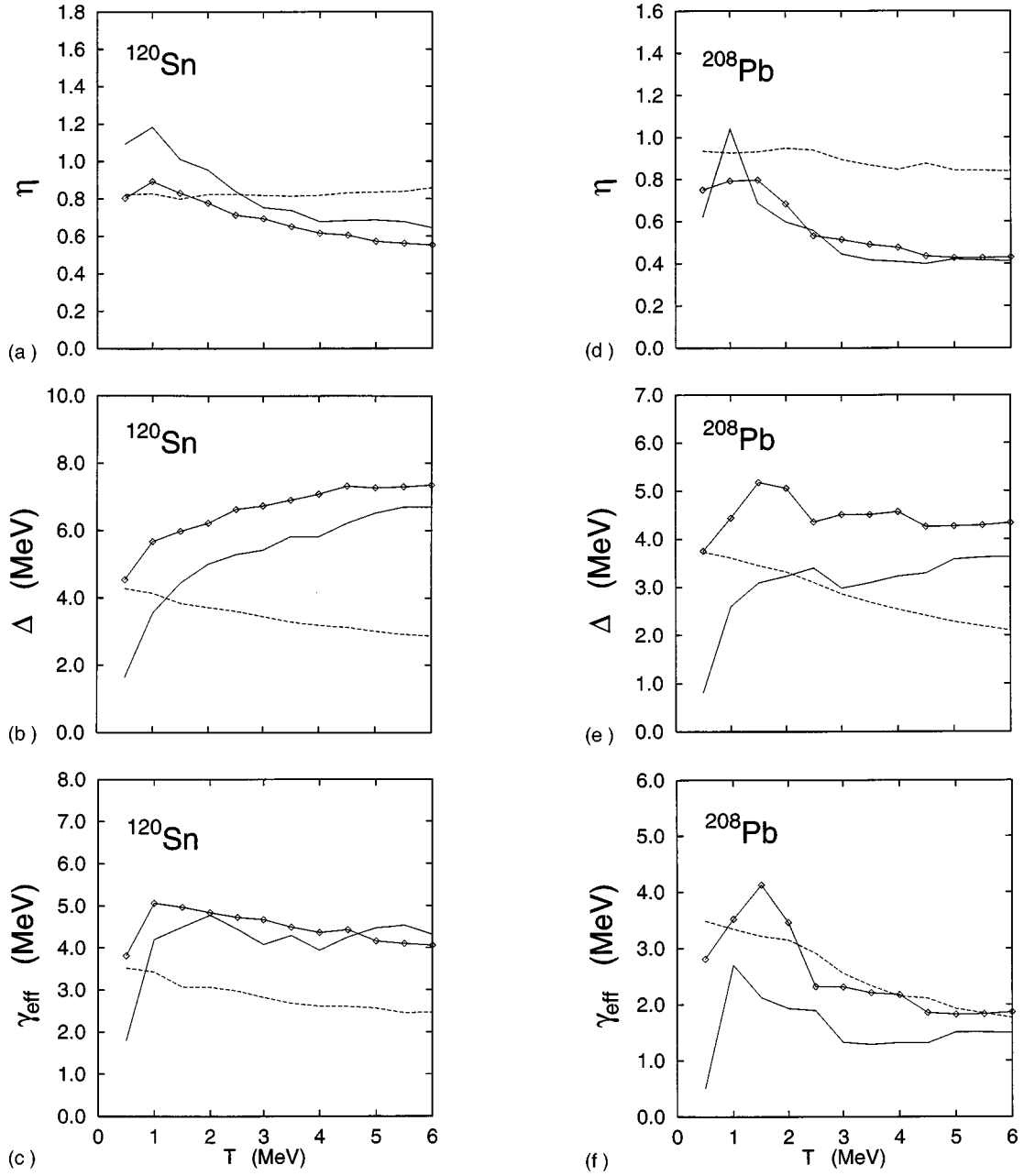

FIG. 7. Adiabaticity parameter η (top), frequency spread Δ (middle), and effective half-width γ_{eff} of the stochastic frequency modulation in the hot GDR as a function of temperature in ^{120}Sn (a)–(c) and ^{208}Pb (d)–(f). The solid curves are the results, obtained via coupling to pp and hh configurations. The dashed curves denote the results, obtained via coupling to only ph configurations. The solid curve with diamonds represents the results obtained via coupling to all ph, pp, and hh configurations.

damping of hot GDR and the macroscopic one for the evolution of the dynamical variable, which describes the evolution of the hot GDR. The microscopic expression for the complex admittance is derived from the Green function, which describes the propagation of the GDR vibration through the field of noncollective degrees of freedom (heat bath).

The present formalism was then applied to a systematic study of the behavior of the GDR as a function of temperature in the nuclei ^{120}Sn and ^{208}Pb. The values of the calculated damping width Γ_{GDR} of the hot GDR, centered at $E_{\text{GDR}}(T)$, were compared with the recent experimental data obtained in the heavy-ion fusion reactions and inelastic α scattering. An overall agreement between theory and experiment is achieved. In comparison to the recent theoretical predictions by other theories in Refs. [18,22,24], the present approach is free from the constraint on adiabaticity and also gives a reasonable agreement with experiments within a much larger temperature interval, including the region of the width's saturation, where the adiabaticity is broken ($\eta < 1$).

The present paper confirms that the thermal effects due to the coupling of the GDR collective vibration to the pp and hh configurations are the source of the increase of the GDR's width at low excitation energies (up to 130–150

MeV) and of the width saturation at high excitation energies. These effects are fairly enough to account for the thermal fluctuations in the hot GDR in finite nuclei. The quantal width Γ_Q due to the coupling of the GDR to only ph configurations decreases slowly with increasing temperature T.

Analyzing the calculated strength distribution of the hot GDR, we see that refined experimental methods are called for to explore the low-energy region of the GDR distribution in order to isolate a possible low-lying structure. In particular, the appearance of the low-lying structure and the difficulties of extracting it from the background are proposed in this work as one possible reason of the ''disappearance'' of the hot GDR in some experiments. On the other hand a more detailed study on the relation between the excitation energy and the temperature in finite nuclei at temperatures below $T=5$ MeV is needed in order to avoid the large uncertainties when comparing theoretical results and the data.

Finally our results seem to indicate the presence of motional narrowing in the hot GDR at $T \geqslant 1$–1.5 MeV as a consequence of the quantal coupling to ph configurations.

ACKNOWLEDGMENTS

Numerical calculations were carried out on a 64 bit Alpha AXP workstation running Digital UNIX (OSF/1) at the Computer Center of RIKEN. Discussions with K. Kumar (Tennessee), Y.Z. Zhuo (Beijing), M. Matsuo (Kyoto), K. Matsuyanagi (Kyoto), N. Onishi (Tokyo), and K. Tanabe (Saitama) are gratefully acknowledged. N.D.D. acknowledges the support from the Nishina Memorial Foundation and the Science and Technology Agency of Japan, under which this work was done.

APPENDIX: RANDOM FREQUENCY MODULATION OF THE HOT GDR AS A STOCHASTIC PROCESS

Motional narrowing as a feature, which takes place in stochastic processes, has been studied by Kubo and Anderson more than four decades ago [54,55]. Recently the Kubo-Anderson process has been applied to study the possibility of motional narrowing in hot nuclei in Ref. [46]. A stochastic macroscopic approach to GDR in hot rotating nuclei has also been developed in Ref. [47] based on the generalized Langevin equation due to Mori [56]. Details of the general theory on motional narrowing in stochastic processes can be found in Ref. [34]. A direct application of this theory to the hot GDR within our model is given in this Appendix.

We have shown that the hot GDR can be considered as a damped oscillator due to the coupling of the collective phonon to the ph, pp, and pp configurations. The broadened frequency spectrum, expressed in terms of the complex admittance or the strength function in Eq. (2.27), is related to the stochastic nature of the time modulation of the phonon energy (the oscillator frequency). In order to study this, we assume that the collective phonon, which generates the hot GDR, is randomly perturbed so that the phonon energy is modulated in time as

$$\omega_q(t)=\omega_q+\omega_q^{(1)}(t), \tag{A1}$$

where the variation $\omega_1(t)$ is a stochastic process. We can write down the equation of motion of the phonon propagation as

$$\dot{Q}_q(t)=i\omega_q(t)Q_q(t). \tag{A2}$$

The solution of Eq. (A2) is

$$Q_q(t)=Q_q(0)\exp\left[i\int_{-\infty}^{t}\omega_q(t')dt'\right]. \tag{A3}$$

The correlation function $\mathcal{F}_q(t)$ for the GDR phonon propagation is directly related to the spectral intensity $J_q(\omega)$ in Eq. (2.30) as

$$\mathcal{F}_q(t)=\langle Q_q^{\dagger}(t)Q_q(0)\rangle=\int_{-\infty}^{\infty}J_q(\omega)e^{i\omega t}d\omega. \tag{A4}$$

Conversely, the spectral intensity is derived from the correlation function via the Fourier transform as

$$J_q(\omega)=\frac{1}{2\pi}\int_{-\infty}^{\infty}\mathcal{F}_q(t)e^{-i\omega t}dt. \tag{A5}$$

If $\omega_q^{(1)}(t)$ is stochastic, then $Q_q(t)$ is a stochastic process defined by Eq. (A2). In this case the correlation function $\mathcal{F}_q(t)$ can be rewritten in the form

$$\begin{aligned}\mathcal{F}_q(t)&=\left\langle Q_q^{\dagger}(0)Q_q(0)\exp\left[i\int_0^t\omega(t')dt'\right]\right\rangle\\&=[\exp(\omega_q/T)-1]^{-1}e^{i\omega_q t}\phi(t),\end{aligned} \tag{A6}$$

where the correlation function $\phi(t)$ is

$$\phi(t)=\left\langle\exp\left[i\int_0^t\omega_q^{(1)}(t')dt'\right]\right\rangle. \tag{A7}$$

Let us define the power spectrum $I(\omega')$ of the stochastic process $\omega_q^{(1)}(t)$, characterizing the frequency modulation, as the Fourier transform of the correlation function $\phi(t)$ as

$$I(\omega')=\frac{1}{2\pi}\int_{-\infty}^{\infty}\phi(t)e^{-i\omega' t}dt, \tag{A8}$$

where

$$\omega'=\omega-\omega_q \tag{A9}$$

is the frequency difference measured from the unperturbed frequency ω_q. Assuming that the process $\omega_q^{(1)}(t)$ is stationary and Gaussian with the average value $\langle\omega_q^{(1)}(t)\rangle=0$, one can define its correlation function from the equation

$$\langle\omega_q^{(1)}(t_0)\omega_1(t_0+t)\rangle=\langle(\omega_q^{(1)})^2\rangle\psi(t). \tag{A10}$$

The correlation function $\phi(t)$ is then related with the relaxation function $\psi(t)$ of this Gaussian stochastic process as

$$\phi(t)=\exp\left[-\langle(\omega_q^{(1)})^2\rangle\int_0^t(t-\tau)\psi(\tau)d\tau\right]. \tag{A11}$$

Substituting $\phi(t)$ in Eq. (A8) with its value from Eq. (A11), one can see that the power spectrum $I(\omega)$ of the stochastic process $\omega_q^{(1)}$ becomes

$$I(\omega)=\frac{1}{2\pi}\int_{-\infty}^{\infty}dt\exp\left[-i\omega t-\Delta^2\int_0^t(t-\tau)\psi(\tau)d\tau\right]. \tag{A12}$$

In Eq. (A12) the quantities

$$\Delta=\sqrt{\langle(\omega_q^{(1)})^2\rangle}, \tag{A13}$$

and

$$\tau_c=\int_0^{\infty}\psi(\tau)d\tau=\frac{1}{\Delta^2}\int_0^{\infty}\langle\omega_1(t_0)\omega_1(t_0+t)\rangle dt \tag{A14}$$

represent the magnitude (spread) and the rate of the random frequency modulation, respectively. This leads to Eq. (2.32), which states that $\tau_c=\Gamma^{-1}$ is just the decay time if the correlation function $\psi(t)$ of $\omega_q^{(1)}$ (or the probability $|\Psi(t)|^2$) exhibits a simple exponential decay as

$$\psi(t)=e^{-t/\tau_c}. \tag{A15}$$

We come to a parameter

$$\eta=\Delta\tau_c=\frac{\sqrt{\langle\omega_1^2\rangle}}{\Gamma}, \tag{A16}$$

which characterizes the behavior of the power spectrum $I(\omega)$ of the stochastic process $\omega_q^{(1)}$. This parameter is called the adiabaticity parameter in Ref. [47], where it was fitted to the experimental data of the hot GDR width within an adiabatic model with shape fluctuations included as in Refs. [16,22,28].

If the exponential decay in Eq. (A15) is assumed, the correlation function $\phi(t)$ in Eq. (A7) becomes

$$\begin{aligned}\phi(t)&=\exp\{-\Delta^2\tau_c[t-\tau_c(1-e^{-t/\tau_c})]\}\\&=\exp[-\eta^2(1/\tau_c-1+e^{-t/\tau_c})].\end{aligned} \tag{A17}$$

In the limit where $\eta\to\infty$ or $\tau_c\to\infty$ the correlation function $\phi(t)$ in Eq. (A17) is approximated by

$$\phi(t)=\exp\left(-\frac{\Delta^2}{2}t^2\right). \tag{A18}$$

The power spectrum $I(\omega)$ of the stochastic process $\omega_q^{(1)}$ then takes a Gaussian form with the standard deviation Δ

$$I(\omega)=\frac{1}{\sqrt{2\pi}\Delta}\exp\left(-\frac{\omega^2}{2\Delta^2}\right). \tag{A19}$$

This power spectrum becomes narrower and narrower when the parameter Δ decreases. This phenomenon is known as motional narrowing. Physically it means that the motion of $Q_q(t)$ in Eq. (A3), which is rewritten as

$$Q_q(t)=Q_q(0)e^{i\omega_q}\exp\left[i\int_{-\infty}^{t}\omega_q^{(1)}(t')dt'\right], \tag{A20}$$

is a Brownian motion on a unit circle in the complex plane. If the duration time is shorter than the characteristic time, needed to maintain a frequency shift,

$$T\simeq\frac{2\pi}{\omega_q^{(1)}}, \tag{A21}$$

the modulation is averaged out and cannot be seen.

In order to derive the clear criteria of motional narrowing we must study the duration time, concerning which there are two extreme cases, namely the short-time ($t/\tau_c\ll1$) and long-time ($t/\tau_c\gg1$) limits.

(a) The short-time limit ($t/\tau_c\ll1$). The short-time limit just corresponds to the approximation in Eqs. (A18) and (A19) when $\eta\gg1$. The correlation function in this case is the average of $\exp(i\omega_q^{(1)})$ over all possible distributions of the modulation $\omega_q^{(1)}$, such as all possible quadrupole shape deformations

$$\phi(t)=\int\exp(i\omega_q^{(1)})\exp[-(\omega_q^{(1)})^2/2\Delta^2]\frac{d\omega_q^{(1)}}{\sqrt{2\pi}\Delta}. \tag{A22}$$

This is an average over an ensemble of oscillators with frequencies $\omega_q^{(1)}$. Each oscillator describes a collective motion during this short time t. In terms of quadrupole shape fluctuations, this dynamical coherent picture takes place if the quadrupole deformation changes slowly enough (τ_c is large enough) for the GDR to feel these changes. Hence the short-time limit here is nothing but *the adiabatic limit* discussed in Ref. [47].

(b) The long-time limit ($t/\tau_c\gg1$). In the long-time limit, which corresponds to $\eta\ll1$, the correlation function $\phi(t)$ in Eq. (A11) behaves as

$$\phi(t)=e^{-\gamma_{\rm eff}|t|+\delta}. \tag{A23}$$

The power spectrum $I(\omega)$ of the stochastic process $\omega_q^{(1)}$ has a good Lorentzian form

$$I(\omega)=\frac{e^{\delta}}{\pi}\frac{\gamma_{\rm eff}}{\omega^2+\gamma_{\rm eff}{}^2}, \tag{A24}$$

where the effective half-width $\gamma_{\rm eff}$ is equal to

$$\gamma_{\rm eff}=\Delta^2\tau_c=\eta\Delta\ll\Delta, \tag{A25}$$

and

$$\delta=\Delta^2\int_0^{\infty}\tau\psi(\tau)d\tau. \tag{A26}$$

This long-time limit was called *the sudden limit* in Ref. [47]. The effective half-width $\gamma_{\rm eff}$ of the power spectrum $I(\omega)$ in the sudden limit (long-time) becomes much smaller than the standard deviation Δ of the Gaussian in the adiabatic (short-time) limit. Hence the sudden limit (long-time limit) is the

region where motional narrowing may start to show up. As such motional narrowing is incompatible with the adiabatic approximation (short-time limit). The recent adiabatic-coupling calculations in Ref. [22], which did not present any evidence of motional narrowing, is a good confirmation of this conclusion. At $T \neq 0$ all the quantities η, Δ, and $\gamma_{\rm eff}$ depend on T. Therefore the criteria (i)–(iii) of motional narrowing, mentioned in Sec. II, are given as a function of temperature. In this way one can clearly point out the temperature region where motional narrowing takes place.

[1] J. J. Gaardhøje *et al.*, Phys. Rev. Lett. **53**, 148 (1984); **56**, 1783 (1986).
[2] J. J. Gaardhøje *et al.*, Phys. Rev. Lett. **59**, 1409 (1987).
[3] D. R. Chakrabarty *et al.*, Phys. Rev. C **36**, 1886 (1987).
[4] A. Bracco *et al.*, Phys. Rev. Lett. **62**, 2080 (1989).
[5] J. H. Le Faou *et al.*, Phys. Rev. Lett. **72**, 3321 (1994).
[6] D. Perroutsakou *et al.*, Nucl. Phys. **A600**, 131 (1996).
[7] K. Snover, Annu. Rev. Nucl. Part. Sci. **36**, 545 (1986); J. J. Gaardhøje, *ibid.* **42**, 483 (1992).
[8] J. L. Egido and P. Ring, J. Phys. G **19**, 1 (1993).
[9] A. V. Ignatyuk, Izv. Akad. Nauk SSSR, Ser. Fiz. **38**, 2613 (1974); A. V. Ignatyuk, *Statistical Properties of Excited Atomic Nuclei* (Energoatomizdat, Moscow, 1983).
[10] H. M. Sommermann, Ann. Phys. (N.Y.) **151**, 163 (1983).
[11] D. Vautherin and N. Vinh Mau, Phys. Lett. **120B**, 261 (1983); Nucl. Phys. **A422**, 140 (1984).
[12] H. Sagawa and G. F. Bertsch, Phys. Lett. **146B**, 138 (1984).
[13] N. Dinh Dang, J. Phys. G **11**, L125 (1985).
[14] P. F. Bortignon *et al.*, Nucl. Phys. **A460**, 149 (1986).
[15] N. Dinh Dang, Nucl. Phys. **A504**, 143 (1989).
[16] M. Gallardo *et al.*, Nucl. Phys. **A443**, 415 (1985); J. M. Pacheco, C. Yannouleas, and R. Broglia, Phys. Rev. Lett. **61**, 294 (1988); Y. Alhassid, B. Bush, and S. Levit, *ibid.* **61**, 1926 (1988).
[17] N. Dinh Dang, J. Phys. G **16**, 623 (1990).
[18] R. A. Broglia, P. F. Bortignon, and A. Bracco, Prog. Part. Nucl. Phys. **28**, 517 (1992).
[19] Ph. Chomaz, Phys. Lett. B **347**, 1 (1995).
[20] A. Bracco *et al.*, Phys. Rev. Lett. **74**, 3748 (1995).
[21] E. Ramakrishnan *et al.*, Phys. Rev. Lett. **76**, 2025 (1996).
[22] W. E. Ormand, P. F. Bortignon, and R. A. Broglia, Phys. Rev. Lett. **77**, 607 (1996); W. E. Ormand *et al.*, Nucl. Phys. **A614**, 217 (1997).
[23] L. D. Landau, Sov. Phys. JETP **5**, 101 (1957).
[24] A. Bonasera *et al.*, Nucl. Phys. **A569**, 215c (1994).
[25] V. Baran *et al.*, Nucl. Phys. **A599**, 29c (1996).
[26] K. Yoshida *et al.*, Phys. Lett. B **245**, 7 (1990); J. Kasagi and K. Yoshida, Nucl. Phys. **A569**, 195 (1994).
[27] V. M. Kolomietz, V. A. Plujko, and S. Shlomo, Phys. Rev. C **52**, 2480 (1995).
[28] Y. Alhassid, B. Bush, and S. Levit, Phys. Rev. Lett. **61**, 1926 (1988); Y. Alhassid and B. Bush, Nucl. Phys. **A531**, 1 (1991); **A531**, 39 (1991); B. Bush and Y. Alhassid, *ibid.* **A531**, 27 (1991).
[29] N. Dinh Dang, in *Proceedings of the Second European Biennal Conference on Nuclear Physics*, Megève, France, 1993, edited by D. Guinet (World Scientific, Singapore, 1995), p. 155; N. Dinh Dang and M. Baldo, in *Proceedings of the Perspectives of Nuclear Physics in the Late Nineties*, Hanoi, Vietnam, 1994, edited by N. Dinh Dang *et al.* (World Scientific, Singapore, 1995), p. 212; N. Dinh Dang, Phys. Rep. **264**, 123 (1996).
[30] N. Dinh Dang and F. Sakata, Phys. Rev. C **55**, 2872 (1997).
[31] N. Dinh Dang and A. Arima, ''Quantal and Thermal Damping of Giant Dipole Resonance in ^{90}Zr, ^{120}Sn, and ^{208}Pb,'' Phys. Rev. Lett. (to be published).
[32] J. Okolowicz *et al.*, Nucl. Phys. **A501**, 289 (1989).
[33] D. N. Zubarev, Sov. Phys. Usp. **3**, 320 (1960).
[34] R. Kubo, M. Toda, and N. Hashitsume, *Statistical Physics II—Nonequilibrium Statistical Mechanics* (Springer, Heidelberg, 1985).
[35] V.G. Soloviev, *Theory of Atomic Nuclei—Quasiparticles and Phonons* (Energoatomizdat, Moscow, 1989).
[36] G. F. Bertsch, P. F. Bortignon, and R. A. Broglia, Rev. Mod. Phys. **55**, 287 (1983).
[37] D. M. Brink, Nucl. Phys. **4**, 215 (1957); A. V. Ignatyuk and I. N. Mikhailov, Yad. Fiz. **33**, 919 (1981); K. Neergard, Phys. Lett. **110B**, 7 (1982); P. Ring *et al.*, Nucl. Phys. **A419**, 261 (1984).
[38] N. Dinh Dang and V.G. Soloviev, ''JINR Communication,'' Report No. P4-83-325 (Dubna, 1983), p. 14 (*in Russian*).
[39] N. N. Bogolyubov and S. Tyablikov, Sov. Phys. Dokl. **4**, 6 (1959).
[40] A. A. Abrikosov, A. P. Gorkov, and I. E. Dzialoshinsky, *Methods of Quantum Field Theory in Statistical Physics* (Pergamon, New York, 1963).
[41] P. F. Bortignon *et al.*, Phys. Rev. Lett. **67**, 3360 (1991).
[42] S. Levit and Y. Alhassid, Nucl. Phys. **A413**, 439 (1984); Y. Alhassid, J. Zingman, and S. Levit, *ibid.* **A469**, 205 (1987).
[43] J. M. Eisenberg and W. Greiner, *Nuclear Theory* (North-Holland, Amsterdam, 1975), Vol. 1, Chaps. 10 and 11.
[44] F. Catara, N. Dinh Dang, and M. Sambataro, Nucl. Phys. **A579**, 1 (1994).
[45] B. Lauritzen *et al.*, Phys. Lett. B **207**, 238 (1988).
[46] W. E. Ormand *et al.*, Phys. Rev. Lett. **64**, 2254 (1989); **69**, 2905 (1992).
[47] Y. Alhassid and B. Bush, Phys. Rev. Lett. **63**, 2452 (1989).
[48] S. Drożdż *et al.*, Phys. Rep. **197**, 1 (1990).
[49] K. Takayanagi, K. Shimizu, and A. Arima, Nucl. Phys. **A447**, 205 (1988); **A481**, 313 (1988).
[50] V. A. Chepurnov, Sov. J. Nucl. Phys. **6**, 955 (1967); K. Takeuchi and P. A. Moldauer, Phys. Lett. **28B**, 384 (1969); V. G. Soloviev *et al.*, Nucl. Phys. **A228**, 376 (1977).
[51] M. Brach and P. Quentin, Phys. Lett. **52B**, 159 (1974); P. Bonche, S. Levit, and D. Vautherin, Nucl. Phys. **A427**, 278 (1984).
[52] B. L. Berman and S. C. Fultz, Rev. Mod. Phys. **47**, 713 (1975).
[53] N. Dinh Dang, Z. Phys. A **335**, 253 (1989).
[54] R. Kubo, J. Phys. Soc. Jpn. **9**, 935 (1954).
[55] P. W. Anderson and P. R. Weiss, Rev. Mod. Phys. **25**, 269 (1954); P. W. Anderson, J. Phys. Soc. Jpn. **9**, 316 (1954).
[56] H. Mori, Prog. Theor. Phys. **33**, 424 (1965).